The Temperature Dependence of $P680^+$ Reduction in Oxygen-Evolving Photosystem II

Chris Jeans,[‡] Maria J. Schilstra,[§] and David R. Klug*

Molecular Dynamics Group, Department of Chemistry, Imperial College, London, SW7 2AY, United Kingdom

Received October 4, 2001; Revised Manuscript Received February 14, 2002

ABSTRACT: The temperature dependence for the reduction of the oxidized primary electron donor $P680^+$ by the redox active tyrosine Y_Z has been studied in oxygen-evolving photosystem II preparations from spinach. The observed temperature dependence is found to vary markedly with the S-state of the manganese cluster. In the higher oxidation states, S_2 and S_3, sub-microsecond $P680^+$ reduction exhibits activation energies of about 260 meV. In contrast, there is only a small temperature dependence for the sub-microsecond reaction in the S_0 and S_1 states (an activation energy of approximately 50 meV). Slower microsecond components of $P680^+$ reduction show an activation energy of about 250 meV which, within experimental error, is independent of the oxidation state of the Mn cluster. By combining these values with measurements of ΔG for electron transfer, the reorganization energies for each component of $P680^+$ reduction have been calculated. High activation and reorganization energies are found for sub-microsecond $P680^+$ reduction in S_2 and S_3, demonstrating that these electron transfers are coupled to significant reorganization events which do not occur in the presence of the lower S-states. One interpretation of these results is that there is an increase in the net charge on the manganese cluster on the S_1 to S_2 transition which acts as a barrier to electron transfer in the higher S-states. This argues against the electroneutrality requirement for some models of the function of the manganese cluster and hence against a role for Y_Z as a hydrogen abstractor on all S-state transitions. An alternative or additional possibility is that there are proton (or other ion) motions in the sub-microsecond phases in S_2 and S_3 which contribute to the large reorganization energies observed, these motions being absent in the S_0 and S_1 states. Indeed charge accumulation may directly cause the increased reorganization energy.

Photosystem II (PSII)[1] catalyzes the electron-transfer reactions from water to plastoquinone in oxygen-evolving organisms (see *1*−*7* for reviews). The process of water splitting begins with the excitation of the primary electron donor P680 by a photon and the rapid reduction of a pheophytin molecule to form the charge-separated state $P680^+Pheo^-$. $Pheo^-$ transfers its electron to bound plastoquinone Q_A, and finally to the mobile plastoquinone Q_B. Q_B binds two protons along with two electrons from Q_A and diffuses into the thylakoid membrane toward the rest of the photosynthetic electron-transfer chain. Oxidized P680 is reduced on a nanosecond to microsecond time scale by the redox active tyrosine residue Y_Z on the D1 polypeptide of photosystem II. Oxidized Y_Z abstracts electrons from a cluster of four manganese atoms to which substrate water molecules are bound. Successive removal of electrons from the Mn cluster cycles it through a series of S-states, S_0 to S_4, where the subscript indicates the number of oxidizing equivalents stored on the cluster. The S_4 state spontaneously converts to S_0 with the release of O_2. During the S-state cycle, four protons are released on the lumenal side of photosystem II. The proton release stoichiometry is the subject of much debate (see *8, 9* for reviews). The main reason for this is that proton release patterns are strongly preparation and pH dependent, and may show noninteger release patterns due to the additional release of electrostatically produced protons. These are released due to changes in the p*K*s of amino acid side chains which occur in response to charge deposition on or around the Mn cluster. In the dark, all PSII centers are converted to the S_1 state through reactions with a second redox tyrosine Y_D located on the D2 polypeptide and through charge recombinations with the acceptor side (see *10*−*12*).

The reduction kinetics of $P680^+$ are strongly dependent on the redox state of the Mn cluster. It has long been known that the majority of $P680^+$ reduction occurs in a few microseconds in active water oxidizing particles. Kinetic components of about 20 ns in S_0 and S_1 and 50 and 250 ns in S_2 and S_3 were originally observed (*13*). Some longer lived microsecond components were also observed; it was postulated that these were due to inactive particles (*13*−*15*) since the data were insufficient to suggest otherwise. Since then, further work by a number of other groups has demonstrated that the microsecond components show oscillations with the

* To whom correspondence should be addressed. Tel/Fax: (44) 020 7594 5806. E-mail: d.klug@ic.ac.uk.

[‡] Current address: Biochemistry Department, Bristol University, Bristol BS8 1TD, United Kingdom.

[§] Current address: Biocomputation Group, Science and Technology Research Centre, University of Hertfordshire, College Lane, Hatfield, Hertfordshire, AL10 9AB, United Kingdom.

[1] Abbreviations: PSII, photosystem II; P680, the primary electron donor of photosystem II; S_n, redox state of the manganese cluster where n = the number of oxidizing equivalents stored ($n = 0-4$); SMNCB, buffer containing 25 mM MES, pH 6.5, 10 mM NaCl, 5 mM $MgCl_2$, 5 mM $CaCl_2$, and 0.3 M sucrose; Y_Z, the secondary electron donor of PSII, tyrosine 161 of the D1 polypeptide; DCBQ, 2,6-dichlorobenzoquinone.

10.1021/bi0118862 CCC: $22.00
Published on Web 03/09/2002

S-state and therefore are at least in part due to active particles (*16*−*18*). It has been observed by a number of groups that there is no significant deuterium isotope effect on the nanosecond phases of $P680^+$ reduction in particles with an intact manganese cluster (*17, 19, 20*). Recent work has shown that H_2O/D_2O exchange causes a decrease in the reduction rates in the microsecond domain (*17*). This suggests that proton/hydrogen transfer is required to complete the reduction of $P680^+$ through a shift in the $Y_Z \rightleftharpoons P680$ equilibrium. This proton-coupled electron-transfer process has since been confirmed by other researchers (*18, 21*).

The majority of $P680^+$ reduction occurs faster in S_0 and S_1 than in the higher S-states. The original explanation for this was that the accumulation of a positive charge in the Mn cluster upon transition S_1 to S_2 results in a Coulombic attractive force, which slows down the transfer of the electron to $P680^+$ (*13*). This suggests that transitions S_0 to S_1 and S_2 to S_3 do not change the net charge on the cluster, and that S_2 and S_3 are more positive than S_0 and S_1 by one charge. For a 1:1:1:1 pattern of electron release from the complex, this implies a proton release stoichiometry of 1:0:1:2, which agrees with some reports on proton release from some PSII preparations (e.g. *22, 23*), but by no means with all reports (see *8, 9* for discussion).

The rates of the S-state transitions are also highly dependent upon the oxidation state of the Mn cluster, but are significantly slower than those of $P680^+$ reduction. Lifetimes of 3 μs (*24*) to 250 μs (*25*) have been reported for the S_0 to S_1 transition, although a more recent report found a value of 40−60 μs (*26*). The S_1 to S_2 transition has a rate constant of about 85 μs (*26, 27*); the S_2 to S_3 transition has been estimated to have a rate constant ranging from 150 μs (*26*) to 300 μs (*25, 28*). The final transition, S_3 to S_0, has a rate constant of about 750−850 μs in thylakoids (*26, 29*) or about 1.2 ms in PSII membranes (*20, 25, 27*). In PSII core particles, this transition has a rate constant of more than 4 ms (*20, 24, 27*).

Only one group has studied the temperature dependence of $P680^+$ reduction by Y_Z in active PSII particles from spinach (*30, 31*). They reported an activation energy of 10 kJ/mol (100 meV) for the fastest phase, a figure which is widely quoted in the literature (e.g., *4, 32*). This activation energy was reported to be independent of S-state. Mn-depleted PSII has also been the subject of study. Loss of manganese converts the nanosecond phases of $P680^+$ reduction into microsecond ones (*33*−*35*). The observed lifetime ranges from about 2 to 44 μs in chloroplasts and from 7 to 35 μs in PSII cores. Activation energies of 46 kJ/mol (480 meV) at pH 7 in chloroplasts (*34*) or 30 kJ/mol (310 meV) at pH 5 in PSII cores from spinach (*36*) have been reported. To our knowledge, a value for this activation energy in BBYs has not been reported.

The interpretation of the 10 kJ/mol activation energy in oxygen-evolving PSII was that the breaking of a hydrogen bond, probably between the phenol group of Y_Z and a basic group, is occurring during electron transfer (*30*). This certainly seems reasonable, given that Y_Z is hydrogen bonded with D1-His190 (*1, 37*−*42*), although hydrogen bonds in proteins are normally of the order of 20 kJ/mol (see, e.g., *43*, p 175). The reason for the increase in activation energy on loss of the manganese cluster is thought to be due to a loosening of the protein structure, allowing more water into the active site (*44*). This presumably leads to an increase in the reorganization energy, λ (*32*), and a distortion of the hydrogen bonding between Y_Z and His190 (*38*). In the depleted system, the presence of the distorted bond requires a concerted proton and electron transfer to occur for $P680^+$ reduction. This manifests itself as a reduction in the rate of electron transfer, an increase in the activation energy, and an increased pH sensitivity with an apparent p*K* of 7 (*36*) compared with about 5 for the intact system (*15, 37*). There is also a higher kinetic isotope effect on $P680^+$ reduction in Mn-depleted particles: 2.5 compared with <1.1 in intact particles (*36*).

The aim of this paper is to provide a reanalysis of the temperature dependence of $P680^+$ reduction in PSII-enriched membrane fragments from spinach. Microsecond time scales are analyzed alongside the nanosecond phases in order to include those components which represent proton-coupled electron transfer (*17, 21, 37*). Furthermore, the reorganization energies which accompany the electron transfers are calculated, to aid assignment of the physical processes which underlie $P680^+$ reduction. The data presented here strongly disagree with those previously published for this electron-transfer reaction (*30, 31*).

MATERIALS AND METHODS

Materials. Oxygen-evolving PSII-enriched granal membranes (BBYs) were prepared according to the method of (*45*) with the modifications described in (*25*). Typical rates of oxygen evolution measured using a Clark-type oxygen electrode at 25 °C were 500 ± 75 μmol of O_2 (mg of chlorophyll)$^{-1}$ h^{-1}. These rates were measured at 5 μg of Chl/mL in buffer containing 25 mM MES, pH 6.5, 10 mM NaCl, 25 mM $CaCl_2$, 0.3 M sucrose, 10 mM $NaHCO_3$, and 5 mM NH_4Cl, in the presence of 1 mM 2,6-dichlorobenzoquinone (DCBQ, Kodak) and 2 mM $K_3Fe(CN)_6$. Manganese depletion of BBYs was achieved by incubating BBYs at 5 mg of Chl/mL at room temperature in SMNCB (25 mM MES, pH 6.5, 10 mM NaCl, 5 mM $MgCl_2$, 5 mM $CaCl_2$, and 0.3 M sucrose) with 50 mM NH_2OH for 5 min. The membranes were pelleted in an eppendorf centrifuge (5 min at 15 000 rpm) and washed once with SMNCB before use.

Equipment. The reduction of $P680^+$ formed by a flash from a Q-switched frequency-doubled Nd:YAG laser (Continuum Surelite, $\lambda = 532$ nm, flash frequency 1−2 Hz, typical pulse energy at sample 10 mJ/cm^2) was probed with nanosecond time resolution at 830 nm by a beam at right angles to the excitation beam. The probe light source was a 35 mW continuous wave diode laser (ML5415N, Mitsubishi). The probe beam was focused onto a photodiode (EG & G FND100). The signal from the photodiode was sent to a 100 MHz oscilloscope (Tektronix TDS 220, 1 Gs/s) and subsequently to a PC via an NI-488.2 instrumentation device and GPIB (National Instruments). Data collection and averaging were carried out using Labview 5.0.1 (National Instruments). Data were collected on two timebases, 2500 channels at 1 ns or 20 ns per channel, giving 2.5 and 50 μs time scales. The instrument response of the system was approximately 10 ns. See (*17*) for full details of the experimental apparatus used.

Samples. BBY samples were diluted to 80 μg of Chl/mL in SMNCB. To reduce light scattering by the membrane

fragments, Triton X-100 was added from a 1% w/v stock solution to a final concentration of 0.016%. This concentration did not affect the kinetics observed; it merely improved the transmission at 830 nm of the sample by preventing aggregation of membranes. The typical transmission of the sample was 80%. The artificial electron acceptor DCBQ was added to a concentration of 100 μM. A fresh stock of DCBQ was prepared prior to each experiment. Samples were typically 250 μL in a 4 mm × 4 mm cuvette. The temperature of the sample was controlled using a combination water-bath and circulator (Haake DC10) and a laboratory built water-jacketed cuvette holder. The temperature in the cuvette was measured using a K-type thermocouple attached to a multimeter which was calibrated against a mercury thermometer.

Data Analysis. Typically 20 sets of 21 flashes were collected and averaged using Labview 5.0.1. Miss factors were calculated according to (*17*). Data for flashes 2−21 were deconvoluted using procedures outlined in (*17, 46*). A global analysis program written and developed in the laboratory ("Look" v. 3.0 by T. Rech and M. Bell) was used to fit the data to multiexponential decays using the Marquardt algorithm for nonlinear least-squares fitting. Typically three or four exponentials and an offset were required to fit the data across both time scales. Global analysis allows the determination of a single set of parameters which fit data collected on different oscilloscope timebases. This ensures that the data can be fitted to the minimum number of exponentials: fitting the data from both time scales separately may result in over-parametrization, due to the presence of microsecond components in the shorter time scale data which can only be resolved accurately in the longer time scale data. The lifetimes arising from such fits correspond to *observed* rates, not intrinsic ones. They are merely a way of describing the kinetics, and should not yet be assumed to be rate constants. This point will be discussed in full as it arises.

RESULTS

Data were collected over a range of temperatures from 5 to 25 °C. Above 25 °C, the kinetics became anomalous and the sample opaque, probably due to aggregation of membrane fragments. The miss factors for the data sets were calculated: these ranged from 14 to 20%, being lowest at 15 °C and increasing as the temperature increased or decreased. Data were deconvoluted as described under Materials and Methods. Figure 1 shows the S-state deconvoluted P680$^+$ reduction kinetics in BBYs from 5 to 25 °C. There is clearly a stronger temperature dependence in the sub-microsecond domain in the S_2 and S_3 states than in the S_0 and S_1 states. At first sight, it appears that the initial amplitude in S_0 and S_1 is lower than in S_2 and S_3. This is a reflection of the faster initial rate constant in the lower S-states. When the response time of the instrumentation (10 ns) is deconvoluted from the data, the initial amplitude is seen to be the same in all S-states; that is, the quantum yield of P680$^+$ formation is independent of S-state (M. J. Schilstra and D. R. Klug, unpublished data). The data presented here have not been corrected for the instrument response, since in all experiments the initial amplitudes observed were highly reproducible. The shift toward lower initial amplitudes at higher temperatures is indicative of an increase in the fastest rate constants, since there is no evidence that the quantum yield of P680$^+$ formation is temperature dependent.

Data for each S-state were globally fitted to a sum of three exponentials and an offset. Amplitudes A_1-A_3 were linked such that they remained constant over the range of temperatures studied, and all lifetimes and the offset were allowed to vary with temperature. Allowing all amplitudes to vary did not significantly improve the quality of the fit ($\chi^2 = 2.21$ for linked A_1-A_3, or $\chi^2 = 2.18$ for all parameters varied, for the S_2 data set). Typical lifetimes and amplitudes at 15 °C are shown in Table 1. The activation energies (ΔE) calculated from Arrhenius plots to the lifetimes resulting from these fits are shown in Table 2. Data were also obtained for Mn-depleted BBYs from 5 to 25 °C (data not shown). These data could be fitted from 1 to 40 μs to the sum of a single exponential and offset of approximately equal amplitude. The activation energy calculated from this fit was 343 ± 42 meV. On longer time scales, these kinetics are clearly multiexponential (see, e.g., *38, 39*), but for the time scale studied here, a single exponential is sufficient to describe the data.

From the data in Figure 1, estimates can be made for the equilibrium constant (K_{eq}) between Y_Z and P680 and hence the free energy gap between these two redox components. After about 40 μs, the reaction has reached a pseudo-equilibrium state. Taking the value of the offset to be the equilibrium concentration of P680$^+$, K_{eq} can be calculated as being [P680]/[P680$^+$], because the reaction is a reduction where P680$^+$ is the reactant and P680 is the product. Therefore:

$$K_{eq} = \frac{([P680^+]_{t=0} - offset)}{offset} \quad (1)$$

Values of the offset were taken from the average amplitude from 40 to 43 μs. The standard free energy gap, $\Delta G°$, was calculated for each temperature according to

$$\Delta G° = -RT \ln K_{eq} \quad (2)$$

This procedure can be taken further. Using a value for the pseudo-equilibrium constant at about 2 μs, we can calculate the $\Delta G°$ associated with the electron transfers which are not rate limited by proton motions (hereafter called $\Delta G°_1$), and the $\Delta G°$ which is associated with the proton-coupled electron transfers ($\Delta G°_2$). In the same way that the overall K was calculated, K_{eq} for the sub-microsecond phases can be calculated from the average amplitude from 2 to 2.5 μs:

$$K_{eq(sub\mu s)} = \frac{([P680^+]_{t=0} - A_{2-2.5\mu s})}{A_{2-2.5\mu s}} \quad (3)$$

It is reasonable to assume this pseudo-equilibrium constant at about 2 μs, since H/D exchange experiments have shown that there is a clear distinction between the nanosecond and microsecond phases (*17, 18, 21*). The average amplitude from 2 to 2.5 μs agrees well with the total amplitude for the microsecond phases calculated from fits to the data, but was found to be more consistent over repeat measurements. The results of these analyses are shown in Table 3. It can be seen that $\Delta G°_1$ varies slightly with temperature, ranging from

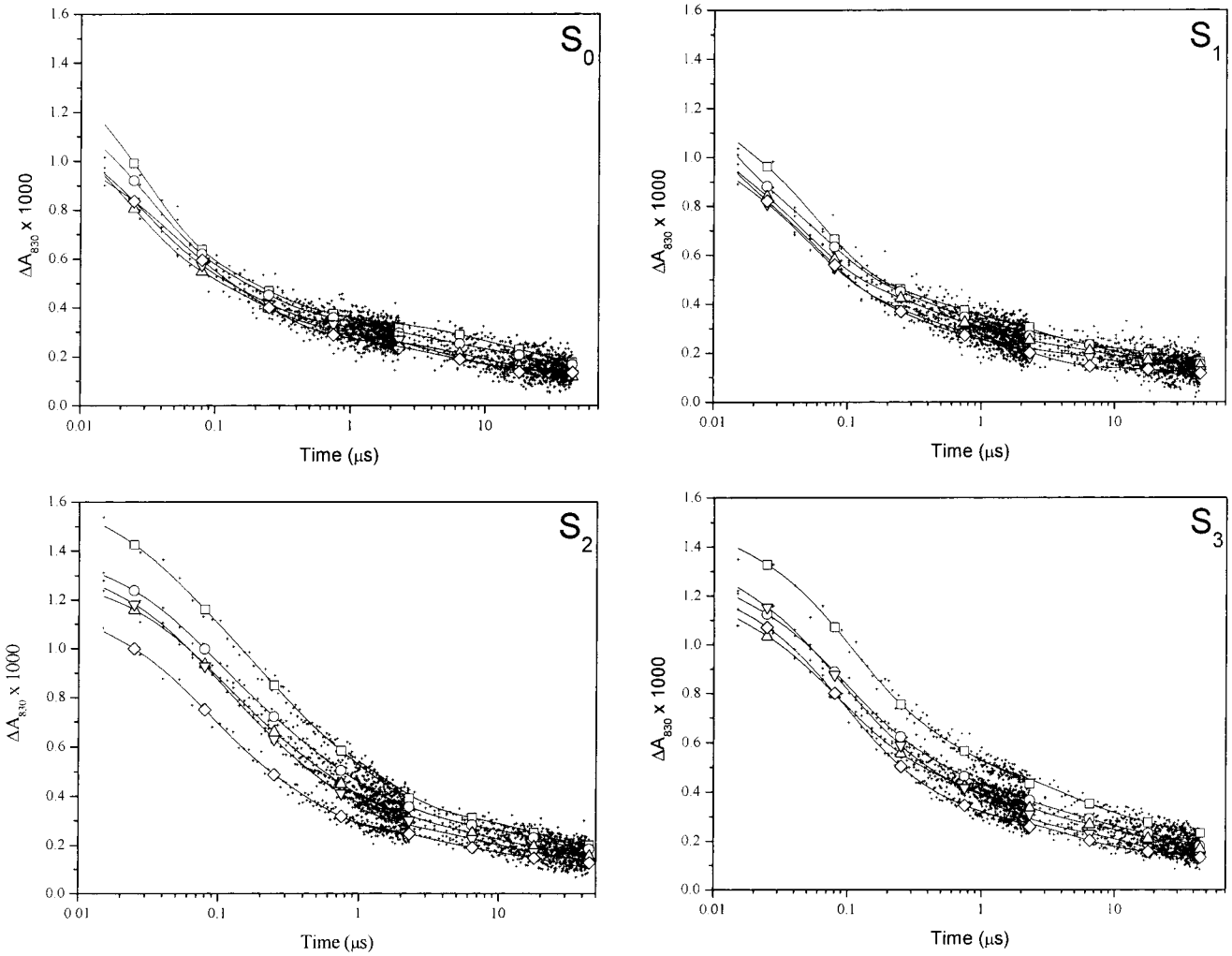

FIGURE 1: S-state deconvoluted $P680^+$ reduction kinetics in BBYs over a range of temperatures. Data are the average of 20 excitations and were collected on two time scales (1 ns/channel and 20 ns/channel). Solid lines represent the best fits of the data to overparametrized multiexponential functions and are indicated merely to guide the eye. Symbols have been plotted to distinguish the curves: 5 °C (squares), 10 °C (circles), 15 °C (up triangles), 20 °C (down triangles), 25 °C (diamonds). For clarity, only one in five actual data points has been shown.

Table 1: Lifetimes of $P680^+$ Reduction in Oxygen-Evolving BBYs Obtained from Global Fits to S-State Deconvoluted Data at 15 °C[a]

S-state	τ_1 (ns)	A_1 (%)	τ_2 (ns)	A_2 (%)	τ_3 (μs)	A_3 (%)	A_4 (%)
S_0	51	53	438	18	11.9	17	12
S_1	56	53	524	18	7.1	14	15
S_2	91	41	624	33	9.1	15	12
S_3	84	51	751	20	12.4	16	13

[a] Data for each S-state were fitted to a sum of three exponentials and an offset. See text for details of fitting procedure.

about −30 to −40 meV. The typical variation in this free energy across the S-states is about 10 meV. The free energy associated with the proton-coupled phases of electron transfer is smaller and less temperature dependent, ranging from about −15 to −20 meV. The typical variation in this free energy across the S-states is less than 5 meV. Although there could be some systematic error in the absolute values of $\Delta G°$, this will largely cancel out in the differences in $\Delta G°$. Even so, errors in the absolute $\Delta G°$s are likely to be small (20% maximum), based on estimation of the maximum concentration of Mn-depleted particles in the sample. We cannot rule out further relaxations on a longer time scale due to recombinations between Q_A^- and $P680^+$ or Y_Z^{ox}.

To be sure that the results obtained from the observed rate constants were comparable to intrinsic rate constants for a simple sequential reaction scheme, the following check was carried out. For a reaction of the A ⇌ B type with a reasonably low equilibrium constant, the observed rate constant (k_{obs}) is the sum of the forward and backward rate constants ($k_+ + k_-$). Hence:

$$k_{obs} = k_+ + k_- \quad (4)$$

$$K_{eq} = \frac{k_+}{k_-} \quad (5)$$

The lifetimes quoted in this paper are only *observed* rate constants. It was necessary to check whether the temperature dependence observed could be due to a temperature effect on K_{eq} according to

$$K_{eq} = A e^{-\Delta G°/k_B T} \quad (6)$$

where A is a preexponential constant and k_B is the Boltzmann constant. The pseudo-equilibrium constant for $P680^+ Y_Z$ ⇌ $P680 Y_Z^{ox}$ is low, of the order of 8−12 at 40 μs, and is

Table 2: Activation Energies (meV) for the First Three Kinetic Components of P680$^+$ Reduction in Oxygen-Evolving BBYs[a]

S-state	τ_1	τ_2	τ_3
S_0	60 ± 100	40 ± 40	270 ± 140
S_1	40 ± 30	70 ± 70	300 ± 50
S_2	250 ± 50	280 ± 50	210 ± 30
S_3	30 ± 60	240 ± 80	220 ± 110

[a] Values were obtained from global fits to S-state deconvoluted data as described in the text. Errors are the standard deviations of fits to the Arrhenius plots.

Table 3: Values of the Standard Free Energy (meV) in the Sub-microsecond Phases ($\Delta G°_1$) and in the Microsecond Phases ($\Delta G°_2$) of P680$^+$ Reduction in Each S-State[a]

temp	$\Delta G°_1$				$\Delta G°_2$			
(°C)	S_0	S_1	S_2	S_3	S_0	S_1	S_2	S_3
5	−34	−36	−30	−28	−16	−16	−19	−19
10	−34	−38	−31	−30	−15	−16	−19	−20
15	−39	−38	−35	−31	−19	−17	−19	−20
20	−40	−49	−38	−35	−22	−11	−24	−22
25	−41	−45	−42	−40	−17	−18	−20	−20

[a] See text for details.

dependent on temperature according to eq 6. Therefore, a change in K_{eq} with temperature may manifest itself as a change in the observed rate constants. This can be addressed by using eqs 4 and 5. Using k_{obs} from fitted data and assuming $K_{eq} = 10$, k_+ was calculated. This showed that k_{obs} provided a fairly constant overestimate of k_+ (data not shown), but that this does not cause a significant error in the calculated activation energy. The difference between $\Delta E(k_{obs})$ and $\Delta E(k_+)$ is within the error from the Arrhenius fits. In conclusion, k_{obs} is an acceptable estimate of k_+, and the observed ΔEs are true activation energies with negligible contributions from the temperature dependence of the equilibrium constant.

DISCUSSION

General. The range of lifetimes for the reduction of P680$^+$ by Y_Z obtained in this report agrees well with the published results of other groups. It is widely agreed that the main component in the sub-microsecond time domain has a lifetime ranging from 20 to 60 ns for S_0 and S_1, while for S_2 and S_3, two nanosecond components of approximately 50 ns and 300 ns lifetimes are seen (*13*−*16*, *30*). These lifetimes are in good agreement with those reported here (Table 1), with the fastest lifetimes being in the range of 40−100 ns, and significantly faster for S_0 and S_1. However, the finding of an early study in which the decay of P680$^+$ in S_1 can be fitted to a single exponential in the nanosecond domain (*13*) is not substantiated here. It seems clear that there are two nanosecond components on all S-state transitions (Table 1). This was also suggested by Lukins et al. (*16*), although no allowance was made for the S-state dependence of the fastest lifetime, nor did they deconvolute their data to correct for misses. Consequently, the 40 ns and the 95 ns lifetimes they observe for each S-state could be due to mixing of the states. The phase of approximately 500 ns seen in S_0 and S_1 is a consistently observed feature which appears regardless of deconvolution parameters or fitting protocols. It is therefore unlikely to be an artifact due to inadequate deconvolution or fitting procedures. It seems reasonable to conclude that there are two components with sub-microsecond lifetimes present in the decay of P680$^+$ in *all* S-states.

The general consensus is that the nanosecond components of P680$^+$ decay correspond to 'pure' electron transfer (electron transfer which is not rate limited by any other processes), while the microsecond components correspond to electron transfer which is rate limited by proton transfer (*17*, *18*). A suggestion to explain the presence of two nanosecond lifetimes in S_2 and S_3 has been proposed (*15*). This took the explanation of the slowing down of the fastest lifetime in the higher S-states being due to Coulombic attraction one step further to explain the biphasic nature of the decay in S_2. The suggestion is that the protonation state of a group with a pK_a of 5.3 within the reaction center leads to a discrete inhomogeneity, in which some of the electron transfer occurs on a tens of nanoseconds time scale, and some on a hundreds of nanoseconds time scale. This explanation is reasonable, but implies that the protonatable group is only present in the higher S-states, whereas the data presented here, showing two sub-microsecond phases in each S-state, imply that such a group would be present in all S-states. Additionally, this group has not been identified, although it is unlikely to be D1-His190 since changes in the protonation state of this residue convert nanosecond phases to microsecond ones (see, e.g., *38*, *39*). In the absence of an identifiable group, no firm conclusions can be drawn. The possibility of internal proton motions on a sub-microsecond time scale cannot be ruled out; these could theoretically be responsible for this biphasicity: although no kinetic isotope effect has ever been observed in these phases (*17*, *19*, *20*), this only means that proton motions are not rate limiting the electron transfer. A reaction in which proton motions occur which are not rate limiting for the electron-transfer step need not show a kinetic isotope effect. Proton motions could still affect the rate of reaction, however, via the reorganization energy. The reorganization energy dictates the curvatures of the reactant and product free energy surfaces (*47*). In this instance, switching from H_2O to D_2O would not affect these curvatures, since the parameters of the free energy surfaces are statistical in nature. A proton motion which occurs faster than the electron transfer will be averaged over all the modes which go to make up the free energy surface. Consequently, the slight change in mass from hydrogen to deuterium would not affect the reorganization energy. Unfortunately, we cannot determine whether a measured reorganization energy arises from proton (or other ion) motions, or from the whole protein's response to charge rearrangements due to the electron-transfer event.

Temperature Dependence. The temperature dependence of P680$^+$ reduction is dominated by the S_2 and S_3 states, especially in the sub-microsecond time domain (Figure 1 and Table 2). This means that upon the S_1 to S_2 transition, there is some kind of change on the donor side which causes P680$^+$ reduction to become more temperature dependent. Upon the S_3 to S_0 transition, this change is reversed. Such a change need not be purely structural, but could involve changes in charge accumulation or distribution, or protonation/deprotonation reactions. These results disagree with previously published data (*30*, *31*, see the introduction). However, these earlier reports are flawed in four ways. First, the data itself are of a rather low signal/noise ratio, presumably due to limitations of the equipment available at the time. Second,

Table 4: Calculated Values of λ (meV) for Each S-State for the Sub-microsecond Phases of $P680^+$ Reduction ($\lambda_{sub\mu s}$) and for the Microsecond Phases ($\lambda_{\mu s}$)[a]

S-state	$\lambda_{sub\mu s}$	$\lambda_{\mu s}$
S_0	270 ± 210	1116 ± 560
S_1	296 ± 150	1232 ± 200
S_2	1130 ± 140	880 ± 120
S_3	1025 ± 170	920 ± 440

[a] See text for details of calculation method.

only the decays following the first flash were included in the analysis. The first flash tends to have anomalous kinetics which are probably due to the presence of centers which only undergo one S-state turnover and are then blocked on the acceptor side (*46*). We do not include flash 1 data in out deconvolution procedure. Third, the method of analysis was somewhat limited, only fitting data for the fastest part of the decay to an average rate constant. Full details of the fit, including the precise time domain fitted over and the number of exponentials which fitted the data best rather than using a single rate constant, are not provided. Finally, only data up to about a microsecond were collected, further limiting the ability of the fitting procedures to fully describe the kinetics.

The values of the standard free energies shown in Table 3 agree reasonably well with those of a previous report (*48*), which found a $\Delta G°$ at about 1 μs of -50 meV in S_0 and S_1 and -20 meV in S_2 and S_3. Given that these values were calculated at a different time point than those presented here, it is not surprising that they give slightly different results. The $\Delta G°_1$ values calculated here are about -40 and -30 meV for the lower and higher S-states, respectively, and are in close agreement with this previous report. The values in Table 3 disagree strongly with the values calculated by Brettel et al. (*13*), who calculated a $\Delta G°_{total}$ of -80 meV in S_0 and S_1 and -20 meV in S_2 and S_3. However, they derived values for the equilibrium constant from fitting their data to a model which involved two electron donors between the Mn cluster and P680, rather than the currently accepted single donor, Y_Z.

Equation 7 shows that the reorganization energy is related to the free energy and the activation energy of a reaction (*47*). Since the latter two parameters are observables, the reorganization energy may be calculated.

$$\Delta E = \frac{(\Delta G° + \lambda)^2}{4\lambda} \quad (7)$$

Table 4 shows the calculated λ values for $P680^+$ reduction for the sub-microsecond and microsecond phases in each S-state. The microsecond phases show reorganization energies of about 1 eV, which within the error limits is independent of S-state. This assumes, of course, that this phase has minimal contributions from Mn-depleted particles. The activation energy for $P680^+$ reduction in Mn-depleted BBYs is 343 ± 42 meV, which is close to but not equal to the activation energies observed in the microsecond phases of intact particles (Table 2). The microsecond phases in intact BBYs cannot be entirely due to Mn-depleted particles since they show strong period-4 oscillations (*17*, *18*, *21*). We estimate a maximum of 10% Mn-depleted particles in a BBY preparation from the amplitude of the oscillations observed

Scheme 1

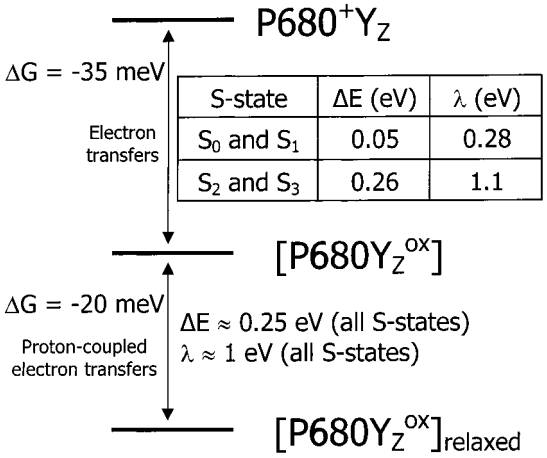

50 μs after excitation, given that the typical amplitude at this time point is 10−12% of the total amplitude, and that the amplitudes of the oscillations about this point are of the order of 1−2% of the total amplitude. The fact that the activation energies for the microsecond phases are, within the error limits, the same for each S-state suggests that the same processes are occurring in these phases regardless of the oxidation state of the Mn cluster. Since proton motions are known to be coupled to these electron transfers (*17*, *18*, *21*), it is reasonable to conclude that the reorganization energies observed for the microsecond phases are due to proton motions and the protein's reorganization to accommodate such motions. Furthermore, the fact that the reorganization energies are roughly equal in each S-state suggests that these proton motions occur to similar extents regardless of the oxidation state of the Mn cluster. The sub-microsecond phases show reorganization energies of over 1 eV in S_2 and S_3, but only about 300 meV in S_0 and S_1. To calculate these values, the average ΔE was used for the S_0, S_1, and S_2 states, since both sub-microsecond phases show similar ΔEs in these states (Table 2). For S_3, ΔE was taken as that for τ_2 (240 ± 80 meV), since the contribution of ΔE for τ_1 in this S-state is negligible in comparison (Table 2). Note that $P680^+$ reduction in S_2 is particularly unique, as all phases of electron transfer are highly temperature dependent. This implies that the events occurring on a sub-hundred nanosecond time scale are likely to be different in S_2 than in the other S-states. The reason for this is not known, but awaits further investigation. The reorganization energies shown in Table 4 are within the range expected for electron transfers between redox centers in relatively polarizable environments (*47*). Scheme 1 shows a summary of the activation and reorganization energies for $P680^+$ reduction by Y_Z.

It is possible to check the approximate validity of the results calculated above. Dutton and co-workers have provided a simple expression which can be used to predict rates of nonadiabatic electron transfer given cofactor to cofactor distance, ΔG, and λ (*49*):

$$\log k_{et} = 13 - [(1.2 - 0.8\rho)(R - 3.6)] - 3.1\frac{(\Delta G + \lambda)^2}{\lambda} \quad (8)$$

where ρ is the packing density, assumed to be 0.75 for most proteins (*49*). From experiments and modeling, the edge-

to-edge distance (R) between P680 and Y_Z has been estimated as 9.5 Å (*32, 50, 51*).

For the sub-microsecond phases of P680$^+$ reduction in S_2 and S_3, eq 8 predicts rate constants of 675 and 328 ns, respectively. The errors in the calculated rate constant are quite large; for S_2, the calculated rate constant one standard deviation below that calculated is 250 ns, and the rate constant one standard deviation above is 1.8 μs. Note that these error bars are asymmetric due to the logarithmic nature of eq 8. The logarithmic nature of the equation also means that reasonably small, e.g., 10%, errors in λ may give up to a 2-fold error in the rate constant. Nonetheless, these calculated rates agree reasonably well with those obtained from fits to the data (Table 1). The predicted rate for the microsecond phases does not agree so well with the observed rate. For an average λ of 1 eV and a $\Delta E°$ of -20 meV, a rate constant of 330 ns is predicted. Discrepancies may be due to nonadiabacity in these reactions due to proton/hydrogen motions or errors in the estimates of the Chl$^+$ to Y_Z distance.

The activation energies for the sub-microsecond phases in the lower S-states range from 40 ± 30 to 60 ± 100 meV, which is in approximate agreement with the value of 100 meV previously reported for S_1 (*30*). Tommos and Babcock used this value to show that eq 8 predicted the correct rate of 20 ns for this electron transfer (*32*), but did not consider the sensitivity of this to errors in the reorganization energy. The calculated λ for S_0 predicts a rate constant of 1 ns (0.4 ns one standard deviation below, 7 ns one standard deviation above). Similar values are obtained for the S_1 state. These values disagree with the observed rate constant by an order of magnitude (Table 1). The reason for this discrepancy is not known. The reorganization energies calculated here show that the events occurring during P680$^+$ reduction on a sub-microsecond time scale are different in S_0 and S_1 than in the higher S-states. In the higher S-states, there is a large reorganization energy associated with the sub-microsecond electron transfer. So what can be happening on the S_1 to S_2 transition to cause Y_Z to P680$^+$ electron transfer to become more temperature dependent?

One possibility has already been proposed. The original explanation for the slower sub-microsecond reduction kinetics of P680$^+$ in S_2 and S_3 was that there is an increase in the net charge on or around the manganese cluster on the S_1 to S_2 transition which is reversed upon the S_3 to S_0 transition. The increased charge retards electron transfer to P680$^+$ in the S_2 and S_3 states by a Coulombic effect (*13*). Although it was not realized at the time, the presence of this extra charge might be expected to affect the degree of reorganization needed following electron transfer, thereby changing the reorganization and activation energies observed. The increased reorganization energies in S_2 and S_3 relative to S_0 and S_1 for the sub-microsecond phases presented in this paper (Table 4) are clearly consistent with this charge accumulation hypothesis. There is good evidence from EXAFS studies that there is no major structural rearrangement on S_1 to S_2 (see *52* for review) and so any changes upon S_2 formation are likely to be charge distribution or hydrogen bonding changes. The problem with this is that the concept of an increased charge on the S_1 to S_2 transition has rather fallen out of favor. This is because although it tied in well with the original proton release data from PSII, further work has shown the proton release pattern to vary significantly with preparation and pH. There is currently much debate over what the intrinsic proton release pattern really is. Additionally, the popular hydrogen abstractor model invokes an electroneutral Mn cluster (*32, 42*). In this model, Y_Z^{ox} abstracts a proton and an electron on each S-state transition. Evidence in support of this model includes EPR experiments showing that Y_Z^{ox} is a neutral radical, at least in Mn-depleted core particles (*53*). As a neutral radical, Y_Z^{ox} could easily accept a hydrogen atom from a donor. The observation that Y_Z is in a mobile and hydrophilic environment relative to Y_D (*41*) suggests that it may play a more complex role, since it might be expected to be held in a fixed position for a pure electron transfer in order to minimize nuclear motions and hence the reorganization energy. That Y_Z is in a hydrophilic environment is also unexpected for an electron-transfer component. Normally, the protein interior for electron transfer would be of a low dielectric constant to provide a small reorganization energy (*41*). The hydrogen bond network is also thought to be more disordered in Y_Z than Y_D (*54, 55*, see also discussion in *41*). The hydrogen abstraction hypothesis was also based upon the fast proton release (12 μs) reported by Haumann and Junge (*56*), which only occurs under nonphysiological conditions of high concentrations of the pH-indicating dye neutral red. Rapid proton release from Y_Z to bulk is needed for the abstracted proton to leave PSII before the next S-state transition occurs, but it has been shown that such proton release is only rapid enough in Mn-depleted particles at low pH (*36*).

So what is the balance of evidence? A recent paper describes the measurement of the proton release pattern from a highly resolved crystallizable oxygen-evolving PSII core particle preparation using a pH electrode (*23*). This technique eliminates artifacts which can arise from the use of pH-indicating dyes such as neutral red, which accumulate at biological membranes (*57*), and which affect the observed proton release depending upon their concentration (see *9*). The pH electrode data show an oscillating pattern of 1:0:1:2, and it seems likely that this represents the true proton release pattern from substrate water. In less resolved preparations, or at varying pHs, this pattern is mixed with electrostatic deprotonations.

If this 1:0:1:2 pattern is that of protons from substrate water, then there probably is charge accumulation on S_1 to S_2. Chloride is essential for the S_2 to S_3 and S_3 to S_0 transitions (*58*), and it has been proposed that chloride may act as a counterion, moving in response to charge movements to maintain *local* electroneutrality (*42*), although as a whole, the Mn cluster has an increased net charge. The hydrogen abstraction model is confusing in this respect, as it invokes chloride motions on these transitions without explaining why this is necessary if no charge accumulation is occurring. A 1:0:1:2 proton release pattern is also suggested on the basis of oscillations of the electrochromic shift (*59, 60*). A recently proposed alternative model for water oxidation shows that the 1:0:1:2 proton release pattern can fit experimental data just as well as a 1:1:1:1 pattern (*61*).

To summarize, the results presented in this paper can be explained by the proposal that there is net charge accumulation upon the S_1 to S_2 transition, which alters the parameters for electron transfer from Y_Z to P680$^+$, resulting in a temperature dependence for this reaction which is not seen

in the lower S-states. This is observed in the previously unstudied phases with lifetimes of several hundred nanoseconds. The implication of these results is that the Mn cluster does not remain electroneutral, that there is a 1:0:1:2 pattern of substrate proton release, and therefore there cannot be hydrogen atom abstraction on each S-state transition. At the moment, we cannot say whether the increase in reorganization energy we observe is due to protein relaxations in response to charge accumulation, or if it actually involves proton (or other ion) movements which are undetectable by hydrogen/deuterium exchange experiments.

Up until now, evidence in support of the charge accumulation hypothesis has come from indirect sources such as the pattern of proton release. To further investigate the possibility of charge accumulation in the cluster, refinement or agreement on the normal proton release pattern would be a helpful starting point. Site-directed mutagenesis may make some contributions, particularly once the crystal structure of PSII (*51*) becomes more highly resolved, and potential ligands to the Mn, Ca, and Cl atoms are identified. Mutants may be found which can assemble the cluster but which show altered oscillation patterns of proton release, $P680^+$ reduction, and so on. This could identify them as possible players in the motion of charges around the cluster during the S-state cycle.

Conclusion. The temperature dependence of $P680^+$ reduction by Y_Z is highly dependent upon the S-state. The S_2 and S_3 states have a far greater activation energy for electron transfer (260 meV) than the S_0 and S_1 states (50 meV). We conclude that this is most likely indicative of an increase in the net charge of the manganese cluster on the S_1 to S_2 transition which is then reversed upon S_3 to S_0. It may alternatively represent the motion of positive ions such as protons to neutralize this accumulation, which is then exhibited via different reorganization energies. This implies that the manganese cluster does not remain electroneutral during the S-state cycle. This is inconsistent with the hydrogen abstraction model for water oxidation.

REFERENCES

1. Britt, R. D. (1996) in *Oxygenic Photosynthesis: The Light Reactions* (Ort, D. R., and Yocum, C. F., Eds.) pp 137−164, Kluwer Academic Publishers, Dordrecht, The Netherlands.
2. Diner, B. A., and Babcock, G. T. (1996) in *Oxygenic Photosynthesis: the light reactions* (Ort, D. R., and Yocum, C. F., Eds.) pp 213−247, Kluwer Academic Publishers, Dordrecht, The Netherlands.
3. Nugent, J. H. A. (1996) *Eur. J. Biochem. 237*, 519−531.
4. Debus, R. J. (1992) *Biochim. Biophys. Acta 1102*, 269−352.
5. Debus, R. J. (2000) in *Metal Ions in Biological Systems* (Sigel, A., and Sigel, H., Eds.) pp 657−711, Marcel Dekker Inc., New York.
6. Nugent, J. H. A., Rich, A. M., and Evans, M. C. W. (2001) *Biochim. Biophys. Acta 1503*, 138−146.
7. Renger, G. (2001) *Biochim. Biophys. Acta 1503*, 210−228.
8. Lavergne, J., and Junge, W. (1993) *Photosynth. Res. 38*, 279−296.
9. Haumann, M., and Junge, W. (1996) in *Oxygenic Photosynthesis: the light reactions* (Ort, D. R., and Yocum, C. F., Eds.) pp 165−192, Kluwer Academic Publishers, Dordrecht, The Netherlands.
10. Vass, I., Deak, Z., and Hindeg, E. (1990) *Biochim. Biophys. Acta 1017*, 63−69.
11. Styring, S., and Rutherford, A. W. (1987) *Biochemistry 26*, 2401−2405.
12. Vass, I., and Styring, S. (1991) *Biochemistry 30*, 830−839.
13. Brettel, K., Schlodder, E., and Witt, H. T. (1984) *Biochim. Biophys. Acta 766*, 403−415.
14. Schlodder, E., Brettel, K., Schatz, G. H., and Witt, H. T. (1984) *Biochim. Biophys. Acta 765*, 178−185.
15. Meyer, B., Schlodder, E., Dekker, J., and Witt, H. (1989) *Biochim. Biophys. Acta 974*, 36−43.
16. Lukins, P. B., Post, A., Walker, P. J., and Larkum, A. W. D. (1996) *Photosynth. Res. 49*, 209−221.
17. Schilstra, M. J., Rappaport, F., Nugent, J. H. A., Barnett, C. J., and Klug, D. R. (1998) *Biochemistry 37*, 3974−3981.
18. Christen, G., Reifarth, F., and Renger, G. (1998) *FEBS Lett. 429*, 49−52.
19. Karge, M., Irrgang, K.-D., Sellin, S., Feinaugle, R., Liu, B., Eckert, H.-J., Eichler, H. J., and Renger, G. (1996) *FEBS Lett. 378*, 140−144.
20. Haumann, M., Bogershausen, O., Cherepanov, D., Ahlbrink, R., and Junge, W. (1997) *Photosynth. Res. 51*, 193−208.
21. Christen, G., and Renger, G. (1999) *Biochemistry 38*, 2068−2077.
22. Forster, V., and Junge, W. (1985) *Photochem. Photobiol. 41*, 183−190.
23. Schlodder, E., and Witt, H. T. (1999) *J. Biol. Chem. 274*, 30387−30392.
24. van Leeuwen, P. J., Heimann, C., Gast, P., Dekker, J. P., and van Gorkom, J. J. (1993) *Photosynth. Res. 38*, 169−176.
25. Rappaport, F., Blanchard-Desce, M., and Lavergne, J. (1994) *Biochim. Biophys. Acta 1184*, 178−192.
26. Razeghifard, M., Klughammer, C., and Pace, R. (1997) *Biochemistry 36*, 86−92.
27. Karge, M., Irrgang, K.-D., and Renger, G. (1997) *Biochemistry 36*, 8904−8913.
28. Dekker, J., Plijter, J., Ouwenand, L., and van Gorkom, H. (1984) *Biochim. Biophys. Acta 767*, 176−179.
29. Razeghifard, M. R., and Pace, R. J. (1999) *Biochemistry 38*, 1252−1257.
30. Eckert, H.-J., and Renger, G. (1988) *FEBS Lett. 236*, 425−431.
31. Renger, G., Eckert, H.-J., Hagemann, R., Hanssum, B., Koike, H., and Wacker, U. (1988) in *Photosynthesis: molecular biology and bioenergetics* (Singhal, S., Ed.) pp 355−371, Nerosa Publishing House, New Delhi.
32. Tommos, C., and Babcock, G. T. (2000) *Biochim. Biophys. Acta 1458*, 199−219.
33. Conjeaud, H., and Mathis, P. (1980) *Biochim. Biophys. Acta 590*, 353−359.
34. Reinman, S., and Mathis, P. (1981) *Biochim. Biophys. Acta 635*, 249−258.
35. Renger, G., and Eckert, H.-J. (1981) *Biochim. Biophys. Acta 638*, 161−171.
36. Ahlbrink, R., Haumann, M., Cherepanov, D., Bogershausen, O., Mulkidjanian, A., and Junge, W. (1998) *Biochemistry 37*, 1131−1142.
37. Christen, G., Seeliger, A., and Renger, G. (1999) *Biochemistry 38*, 6082−6092.
38. Hays, A.-M. A., Vassiliev, I. R., Golbeck, J. H., and Debus, R. J. (1998) *Biochemistry 37*, 11352−11365.
39. Hays, A.-M. A., Vassiliev, I. R., Golbeck, J. H., and Debus, R. J. (1999) *Biochemistry 38*, 11851−11865.
40. Haumann, M., Mulkidjanian, A., and Junge, W. (1999) *Biochemistry 38*, 1258−1267.
41. Hoganson, C. W., Lydakis-Simantiris, N., Tang, X.-S., Tommos, C., Warnke, K., Babcock, G. T., Diner, B. A., McCracken, J., and Styring, S. (1995) *Photosynth. Res. 46*, 177−184.
42. Tommos, C., and Babcock, G. T. (1998) *Acc. Chem. Res. 31*, 18−25.
43. Voet, D., and Voet, J. G. (1990) *Biochemistry*, John Wiley and Sons, New York.
44. Wydrzynski, T., Hillier, W., and Messinger, J. (1996) *Physiol. Plant. 96*, 342−350.
45. Berthold, D. A., Babcock, G. T., and Yocum, C. F. (1981) *FEBS Lett. 134*, 231−234.
46. Lavergne, J. (1991) *Biochim. Biophys. Acta 1060*, 175−188.

47. Moser, C. C., and Dutton, P. L. (1996) in *Protein Electron Transfer* (Bendall, D. S., Ed.) pp 1−21, BIOS Scientific Publishers Ltd., Oxford, England.
48. Rappaport, F., Porter, G., Barber, J., Klug, D., and Lavergne, J. (1995) in *Photosynthesis: from light to biosphere* (Mathis, P., Ed.) pp 345−348, Kluwer Academic Publishers, Montpelier.
49. Page, C. C., Moser, C. C., Chen, X., and Dutton, P. L. (1999) *Nature 402*, 47−52.
50. Svensson, B., Etchebest, C., Tuffery, P., van Kan, P., Smith, J., and Styring, S. (1996) *Biochemistry 35*, 14486−14502.
51. Zouni, A., Witt, H.-T., Kern, J., Fromme, P., Kraus, N., Saenger, W., and Ort, P. (2001) *Nature 409*, 739−743.
52. Pecoraro, V. L., and Hsieh, W.-Y. (2000) in *Metal Ions in Biological Systems* (Sigel, A., and Sigel, H., Eds.) pp 429−504, Marcel Dekker Inc., New York.
53. Gilchrist, M. L., Ball, J. A., Randall, D. W., and Britt, R. D. (1995) *Proc. Natl. Acad. Sci. U.S.A. 92*, 9545−9549.
54. Tommos, C., Tang, X.-S., Warncke, K., Hoganson, C. W., Styring, S., McCracken, J., Diner, B. A., and Babcock, G. T. (1995) *J. Am. Chem. Soc. 117*, 10325−10335.
55. Tang, X.-S., Zheng, M., Chisholm, D. A., Dismukes, G. C., and Diner, B. A. (1996) *Biochemistry 35*, 1475−1484.
56. Haumann, M., and Junge, W. (1994) *Biochemistry 33*, 864−872.
57. Hong, Y. Q., and Junge, W. (1983) *Biochim. Biophys. Acta 722*, 197−208.
58. Wincencjusz, H., van Gorkom, H. J., and Yocum, C. F. (1997) *Biochemistry 36*, 3663−3670.
59. Saygin, O., and Witt, H. T. (1984) *FEBS Lett. 176*, 83−87.
60. Saygin, O., and Witt, H. T. (1985) *FEBS Lett. 187*, 224−226.
61. Messinger, J. (2000) *Biochim. Biophys. Acta 1459*, 481−288.

BI0118862